Paper No.
05421

CORROSION 2005

Selection of High Performance Alloys for High Temperature Corrosion Environments

D. L. Klarstrom and S. K. Srivastava
Haynes International, Inc.
Kokomo, IN 46904-9013

ABSTRACT

High temperature gaseous environments that promote corrosion attack are present in a variety of industrial environments such as chemical and petrochemical processing, glass manufacturing, waste incineration, cement manufacture, mineral processing and metals heat treatment and finishing. These aggressive environments can involve corrosive attack in the forms of oxidation, sulfidation, nitridation, carburization, metal dusting, chlorination and molten salt corrosion. The paper will discuss the selection of the correct alloy(s) to withstand each type of environment.

Keywords: Nickel alloys, oxidation, sulfidation, nitridation, carburization, metal dusting, chlorination, molten salt corrosion

INTRODUCTION

Nickel-base alloys are industrially important for their resistance to certain types of high temperature corrosion. For example, they have outstanding resistance to oxidation, and they are generally superior to iron- or cobalt-base alloys in this mode of attack. They have low solubilities for interstitial atoms, which makes them inherently more resistant to carburization and nitridation attack than other alloy bases. They also have good resistance to halogen-containing environments due to the high melting points of the halogen compounds formed. A summary of the nominal compositions of some alloys resistant to various forms of high temperature corrosion is given in Table 1.

The Ni-Cr-Fe family consists of general purpose type materials that are used in a wide variety of applications because of their good resistance to many forms of high temperature corrosion and more reasonable costs. The Ni-Cr-Fe-Al family can be viewed as an upgrade over the Ni-Cr-Fe alloys through the use of Al additions to enhance their resistance to high temperature corrosion by making use of Al_2O_3 formation. For 601 and 693 alloys, this occurs in the form of sub-surface oxides. On the other hand, enough Al is present in 214™ (A) alloy

so that a complete Al_2O_3 film can form on its surface to serve as a barrier to the corrosive species. The Ni-Cr-Mo/W alloy family consists of materials which have very good high temperature strength in addition to resistance to certain forms of high temperature corrosion. Therefore, they are used in a great variety of high temperature structural components. Finally, the Ni-Co-Cr-Si category, consisting of HR-160® alloy, represents a unique material that resists high temperature sulfidation as well as environments containing complex mixed salts through critical additions of Co, Cr and Si. This alloy is unusual since nickel-base alloys are not noted for their resistance to sulfidation attack.

In the sections to follow, the resistance of these nickel-base alloys to a variety of high temperature corrosion modes of attack will be described in detail. These modes include oxidation, carburization, metal dusting, sulfidation, nitridation, halogens and molten salts.

HIGH TEMPERATURE CORROSION PROPERTIES

Oxidation

To provide resistance to high temperature oxidation, most of the nickel-base alloys rely on additions of chromium. As shown in Table 1, the levels range from 8-29%. Some of the alloys contain minor additions of silicon and manganese to promote the formation of highly protective spinel oxides. Additions of rare earth elements such as lanthanum and yttrium can also be used to enhance the resistance of the oxide scales to spallation. Some of the alloys have additions of aluminum on order to form Al_2O_3. However, these occur as subsurface scales beneath the Cr_2O_3 oxide that forms first. If sufficient aluminum is present, as in the case of 214 alloy, then a continuous Al_2O_3 layer can form on the surface. The growth of this oxide is very slow at low temperatures (<900°C), so NiO and Cr_2O_3 oxides are formed initially, and the Al_2O_3 layer is formed beneath them. At temperatures of 1000°C and above, the growth kinetics of the oxide are more rapid, and the Al_2O_3 oxide layer is readily formed.

Oxidation attack consists of two major components: (1) a loss of metal as the base material is converted into an oxide scale, and (2) internal attack which may consist of intergranular attack along with isolated internal oxides. The metal loss can further be described in terms of a continuous oxide scale and oxides lost by spallation if thermal cycling is involved. For internal attack, if the exposure is in air, then the formation of internal nitrides can occur along with internal oxides. This is especially the case in Cr_2O_3 forming alloys if significant oxide spallation has taken place, or if the alloy contains insufficient Al to form a continuous Al_2O_3 layer. The characterization of oxidation attack by measurement of weight changes during the exposure does not give a complete description of the damage. Therefore, it is imperative to examine the exposed samples metallographically and make measurements of the observed attack. In the sections to follow, oxidation attack is expressed as the average metal affected which comprises metal loss + average internal attack.

(A) 214™, 230®, HR-120® and HR-160® are trademarks of Haynes International, Inc.

As one might intuitively expect, the degree of oxidation attack generally increases with increasing temperature. This is illustrated in Table 2 for selected nickel-base alloys for tests carried out in flowing air with cycling to room temperature every 168 hours. At temperatures above 980°C, volatile CrO_3 is formed, and the protective value of the Cr_2O_3 scale is degraded. This effect is especially evident in the data for 1205°C. One can also appreciate that an Al_2O_3 oxide layer is highly protective as evidenced by the results shown for 214 alloy. Very low values are noted for all four temperatures.

As stated earlier, cycling to room temperature can have a marked effect on the extent of oxidation attack due to spallation of the oxide scales. This is illustrated by the data shown in Table 3 for flowing air at 1095°C. Even though the lengths of the two tests were similar, the amount of damage for the shorter cycling time was much greater.

The amount of attack is even more severe for conditions representing a high velocity combustion gas and a short cycle time. This type of test was designed to simulate the conditions in a flying gas turbine.[1] The test rig burns a mixture of No. 1 and No. 2 fuel oils with an air to fuel ratio of 50:1 to produce a combustion gas having a velocity of Mach 0.3. The samples are held in a rotating carousel which is withdrawn from the hot zone every 30 minutes and cooled with a blast of air for 2 minutes, after which it is inserted back into the hot zone. Results of such tests at 980 and 1095°C are presented in Table 4. One can appreciate the greater severity of these tests by comparing the results to those shown in Table 2.

A final point to be made about oxidation attack is the effect of time. One should not make a judgment on long term behavior based on the results of short term tests. Some materials can exhibit a phenomenon known as “breakaway oxidation” in a prolonged exposure. For example, the data shown in Table 5 indicate that X and HR-120® alloys suffered catastrophic oxidation attack in long term tests carried out at 1205°C. For X alloy, complete failure of the sample occurred in 120 days, and for HR-120 alloy, failure occurred in 330 days. Therefore, the data indicate that neither alloy is suitable for long term service at temperatures above 1150°C.

Carburization

Carburization refers to ingress of carbon into the metal. This phenomenon occurs in many processing industries in the presence of carbonaceous gases such as CO, CO_2, CH_4 and other hydrocarbons. Carbon is transferred to the metal surface, diffuses through the metal and forms various carbides with the alloying elements. It is generally observed at temperatures >800°C and carbon activity < 1. When the temperature is lower and the carbon activity is greater than 1, another mode of corrosion, metal dusting, is observed to occur. Metal dusting is covered in the following section. Carburization is different from most other modes of high temperature corrosion; formation of internal carbides leads to metal degradation, embrittlement and fracture. In this mode, metal loss due to scale formation does not take place; corrosion damage cannot be defined in terms of sum of the metal loss and internal attack. Instead, the magnitude of carburization is defined by the mass carbon pick up (mg/cm2) and the depth of carburization. The kinetics of the carburization depends upon solubility and diffusivity of carbon at the service temperature. The solubility of carbon in nickel alloys is low; therefore, use of nickel alloys is fairly widespread. However, heat resistant alloys invariably contain

many alloying elements, such as chromium, aluminum, silicon, etc. Carburization thus always leads to the formation of various chromium carbides. Carburization is prevented in nickel alloys by the formation of protective and stable oxide scales. Whether an alloy will undergo oxidation or carburization in a gas mixture at the temperature will be determined by the partial pressure of oxygen (oxygen potential) and the carbon activity at the temperature. For an understanding of thermodynamic principles underlying carburization, the reader is referred to the excellent monograph entitled, "Carburization" by Grabke.[2] At higher temperatures, typically greater than 1050°C, oxide scales are stable in the following order: $Al_2O_3 > SiO_2 > Cr_2O_3$. Therefore, for service below 1050°C, chromia forming alloys would offer satisfactory life. For service above 1050°C, silica or alumina forming alloys should be preferred. If the processing conditions alternate with carburizing and oxidizing environments, chromium in the alloy would alternately oxidize and carburize. Carburization of oxides releases CO for subsequent oxidation and the cycle continues. This phenomenon leads to what is known as "green rot" due to the presence of greenish chromium oxides on the fracture surface.

Carburization data for several commercial alloys are given in Table 5.[3] All alloys were tested in a gaseous mixture comprised of 5% H_2, 5%CO, 5%CH_4, and balance Ar (by volume). They were tested at 871°C and 927°C for 215 hours and at 982°C for 55 hours. The environment was characterized by a low oxygen potential and unit carbon activity. While the gaseous composition remained constant, the partial pressures of oxygen changed at different temperatures. The calculated equilibrium oxygen partial pressures at the test temperatures were as follows: at 871°C, $Po_2 = 8.13 \times 10^{-23}$ atma; at 927°C, $Po_2 = 2.47 \times 10^{-22}$ atma; and at 982°C, $Po_2 = 6.78 \times 10^{-22}$ atma. The results are tabulated in Table 6. It can be noted that the magnitude of carbon pick up increased significantly at 982°C, even though the duration of testing was much shorter. Micrographs showing carburization for a set of nickel base alloys at 982°C/55 hours is shown in Figure 1. Carburization leads to degradation of properties. The influence of carburizing exposure on the residual tensile and Charpy impact properties has been reported for a wide variety of alloys by Rothman et al. [4]

Another set of carburization data are reported in Table 7.[5] In this instance, a wide variety of alloys were exposed to a gaseous mixture comprised of 5% H_2, 1% CH_4 and balance Ar (by volume) at 982°C for 55 hours. The results are reported in terms of the mass carbon pick up and also the average internal penetration as well as the maximum internal penetration. The latter two were measured using an optical microscope. The oxygen potential for this environment would be expected to be especially low, as the only source of oxygen would be the impurities present in the gaseous mixture. The carbon activity for this environment equaled one. A cursory examination of the two tables shows that in the second environment, i.e., 5%H2 +1% CH4 + Ar, the magnitude of carbon pick up for the tested materials was much higher than that in the first environment. Apparently, the alloys did not have sufficient oxygen to form a protective scale in this environment. 214 alloy with its alumina rich protective scale showed the least propensity to carburize.

Metal Dusting

Metal dusting is a form of material degradation that occurs in a strongly carburizing environment in which the carbon activity is >>1 and the oxygen partial pressure is very low. It

also mainly occurs in the temperature range of 450°-750°C.[6] The attack generally occurs in Fe-, Ni- and Co-based alloys and results in the formation of a dust composed of metal particles and carbon. Sometimes oxides and carbide particles are included as well. This high temperature corrosion phenomenon is a particular problem in industrial processes such as ethylene pyrolysis, hydrogen reforming, ammonia synthesis and steel surface carburization in which the conditions required for metal dusting are met. A number of studies have been carried out to determine the compositional factors that provide good resistance to this form of attack.[7-9] These studies have resulted in the following guidelines. Nickel-base alloys are favored since their solubility of carbon is relatively low. High chromium levels (22-28%) give better resistance perhaps because a protective oxide film is better able to form in the low oxygen environment. Aluminum additions appear to be beneficial due to the formation of Al_2O_3 films, but in environments having very low oxygen partial pressures, such protective layers cannot be readily formed. It appears that additions of Mo and W are also beneficial probably because they tie up carbon in the form of carbides and, thereby, delay the onset of metal dusting. Finally, additions of silicon have been shown to be effective in resisting metal dusting.

A standardized test for metal dusting has not been developed because the conditions that produce it are quite varied. For nickel-base alloys, the attack has a very long period of incubation which can last many thousands of hours. This is especially true if the levels of iron are low. The progression of the attack has been studied by periodically determining the rate of metal wastage during the test.[6-8] After the incubation period, the rate of metal wastage increases dramatically and may show a slight decrease as illustrated in Figure 2. Eventually, pits may form to signify the onset of the metal dusting process as shown in Figure 3. A summary of metal wastage rates obtained for a very severe metal dusting environment is given in Table 8.

Sulfidation

Nickel sulfides will form in an environment comprised of only H_2 and H_2S. Ni-Ni_3S_2 forms a low temperature eutectic and melts at 635°C. Liquid sulfide products accelerate corrosion rate greatly. As such, nickel alloys would be unsuitable for use in such environments above about 600°C. However, most industrial processing involves sulfidizing and oxidizing environments and comprised of H_2, H_2S, H_2O, SO_2, CO, CO_2, etc. Under these conditions, nickel alloys derive their resistance to sulfidation by the formation of protective oxide scale of chromium, silicon or aluminum. Sulfide scales are not protective. Sulfides contain a high degree of defects, therefore diffusion rates of metal ions through sulfides are much faster. Kinetics of sulfidation, akin to those of oxidation depend upon metal ion diffusion and are parabolic in nature. However, rate constants for sulfidation reaction are several orders of magnitude greater than those for oxidation reaction. Nickel alloys derive their resistance to sulfidation by the formation of a protective oxide scale impervious to the sulfur diffusion or reaction. The main resistance depends upon alloying with chromium. Some alloys also contain significant amounts of aluminum or silicon. The presence of aluminum or silicon may contribute to sulfidation resistance by forming an Al_2O_3 or SiO_2 rich sublayer.

The magnitude of corrosion attack is determined by the environment, the temperature and the duration of the exposure. A thermodynamic analysis is necessary to determine the partial

pressures of sulfur and oxygen to define the environment at a given temperature. The partial pressures of sulfur and oxygen can be used to construct a phase stability diagram for a given metal, which will indicate whether it will form only sulfides, a mixture of sulfides and oxides, or only oxides. For an alloy based on Ni-Cr system, it might be necessary to superimpose the stability diagram for chromium on that for nickel to identify regions of stability for various compounds. Similarly, for an alloy based on Ni-Cr-Si system, superimposition of three phase stability diagrams would be needed to identify the regions of stable phases. For an understanding of the thermochemical principles, the reader is referred to Birks and Meier[10], and Kofstad.[11]

Coal gasification is an important process providing material challenges. T.P. Levi et al.[12] reported an evaluation of alloys exposed to a gaseous environment, typical of coal gasification, comprised of 0.9% CO, 22.2% H_2O, 1.1% H2S and balance H_2 at 600°C. Their results are presented in Table 9. In this test, the prediction of corrosion attack for a one year period showed HR-160 alloy to be the most sulfidation resistant due to the presence of a continuous silica-rich layer which protected the substrate metal. 45TM alloy formed a friable external Fe, Ni and Cr-sulfide scale; the corrosion attack could not be extrapolated. MA956 alloy, an iron based mechanical alloy, formed discontinuous Al-rich oxide scale, which did not offer sufficient protection from sulfidation.

Sulfidation data for tests conducted in a gaseous environment comprising of 5% H_2, 5% CO, 1% CO_2, 0.15% H_2S and balance Ar at 760°C, 871°C and 982°C are reported in Tables 10, 11 and 12.[13] While the gaseous composition was the same at each temperature, it should be observed that partial pressures of sulfur and oxygen did not remain the same. Most of the nickel based alloys were consumed in the test at 760°C. For 671 alloy, the high chromium content provided a protective oxide scale that enhanced its sulfidation resistance. For HR-160 alloy, a silica-rich chromium scale imparted resistance. At 871°C, the partial pressures of sulfur and oxygen changed slightly, and the carbon activity was zero. Many of the nickel alloys were consumed or suffered a high degree of corrosion attack. Of note was the observation that 671 alloy, which suffered only a modest degree of attack in the 215-hr test, was consumed in the 500-hr test.

Sulfidation data for tests in an SO_2 bearing oxidizing environment, 10%SO_2, 5% O_2, 5% CO_2 and balance Ar, at 1093°C are shown in Table 13. The test duration for all tests was 215 hours. The results show that in this environment most of the alloys performed satisfactorily.

In this section, sulfidation data for a variety of nickel alloys were reported for relatively short term, < 500hr., test periods. These results should not be extrapolated to estimate the long-term performance for the alloys. However, the results are useful in discriminating the relative performance of various alloys.

Chlorination

Corrosion by halogens primarily refers to corrosion by gaseous Cl_2/HCl, and it occurs in many industrial environments. Examples include coal combustion (<950°C), mineral chlorination (300-900°C), production of ethylene dichloride (280-480°C), titanium dioxide production

(900°C), waste incineration (~900°C), etc.[14] The amount of chlorine in the environment can range from ~0.01 vol. % in coal combustion to ~2 vol. % in hazardous waste incineration. Corrosion by Cl_2/HCl presents a very challenging problem; in contrast to oxides, metal chlorides are marked by low melting points and high vapor pressures. Relative to many chlorides, the melting points of $NiCl_2$ (1030°C) and $CrCl_3$ (1150°C) are much higher; therefore, nickel alloys with higher nickel and chromium contents are frequently used for corrosion protection in such environments. In the presence of oxygen, the corrosion attack involves the formation of oxides as well as volatile chlorides.

Corrosion data for a variety of commercial nickel alloys tested in Ar-$20O_2$-$0.25Cl_2$ at various temperatures for 400 hours is shown in Table 14.[15-16] The superior resistance of alloy 214 is attributed to the formation of a protective Al_2O_3 scale in this environment. Also, the presence of refractory elements, such as W and Mo, was detrimental to chloridation resistance due to the formation of volatile oxy-chlorides. Both alloy S and C -276 contain significant amounts of Mo and exhibited a poorer response.

Corrosion data for tests run in air + 2%Cl_2 at 900°C and 1000°C for 50 hours is given in Table 15.[17] These results are similar to those for the previous environment. In a series of papers, Schwalm and Schutze have published corrosion behavior of several alloys in air + 2 vol-% Cl_2 at 300 to 800°C.[18] Their results are summarized in Table 16. For all alloys, it was believed that due to lower testing temperatures and/or short periods of testing, protective scale formation did not take place. This behavior makes long term prediction of alloy corrosion resistance in such environments very difficult.

Nickel alloys containing chromium, such as C-4, alloy 625 and 600 possess good resistance to gaseous HCl up to 700°C. Additionally, it has been observed that Ni-Cr-Mo alloys, such as C-276 and S were better than alloy 625, X and 600. Barnes studied corrosion resistance of several alloys in 100% HCl, the results are presented in Table 17.[19] The increase in the corrosion rate for HR-160 alloy at higher temperatures was attributed to the high cobalt content of the alloy.

Corrosion by Molten Salts

The heat treating industry has been using salt pots and heat exchangers containing a variety of molten salts for a long time. They are used extensively for the heat treatment of metals and alloys. The furnace equipment and other containment equipment in contact with the molten salt suffer from high temperature corrosion. Molten salt corrosion is also encountered in heat transfer and energy-storage media used solar energy and nuclear systems, fuel cells, high-temperature batteries, metallurgical extraction processes, etc.

Molten salts flux away the protective oxides scale from a metal surface causing the corrosion to proceed by oxidation of the alloy followed by dissolution of the oxide into the molten salt. The magnitude of oxygen and water vapor present in the molten salts accentuates the kinetics of molten salt corrosion. The heat treating industry uses various compositions of neutral salt in many heat treating operations, such as annealing, quenching, tempering, etc. Examples of

typical salt baths are - 50NaCl – 50KCl, 50KCl – 50Na_2CO_3, 20NaCl – 25KCl – 55$BaCl_2$, 25NaCl – 75$BaCl_2$, 21NaCl – 31$BaCl_2$ – 48$CaCl_2$.

The corrosion results of a field test in NaCl-KCl-$BaCl_2$ at 840°C for one month are shown in Table 18.[20] The mechanism of the corrosion attack was predominantly intergranular. Results of a laboratory testing in a NaCl salt bath at 840°C for 100 h are given in Table 19. Again the corrosion attack was mainly intergranular without discernible metal loss.

In addition to chloride salt baths, molten mixtures of nitrate – nitrite salts are also extensively used in the heat treat industry in the range of 150 – 600°C. Slusser et al.[21] evaluated corrosion of various alloys in an equimolar $NaNO_3$ – KNO_3 salt bath at 675°C for 336 hours, with an equilibrium amount of nitrite concentration. They found a decrease in the corrosion rate with the nickel content of the alloys tested. However, Ni 200 alloy, showed a sharp increase in the corrosion rate. The results of corrosion rates for tests at 675°C and 700°C in the sodium-potassium nitrate-nitrite salt, for two test durations, are shown in Table 20. The corrosion rates appear similar in the two tests. Alloy 800 showed a sharp increase at the higher temperature.

Concluding Remarks

Nickel alloys possess very good resistance to a variety of high temperature corrosion environments. The modes of corrosion attack are specific to each type of environment. Therefore, different alloying additions are required to obtain the best resistance. The information provided should provide a useful reference for the selection of the appropriate alloy.

REFERENCES

1. M. F. Rothman, “Oxidation Resistance of Gas Turbine Combustion Materials,” ASME Paper 85-GT-10, ASME, NY, NY.
2. H.J. Grabke, CARBURIZATION A High Temperature Corrosion Phenomenon, MTI Publications No. 52, 1998, MTI, St. Louis, MO.
3. George Y. Lai, Carburization Resistance of Commercial Wrought Alloys, R & D Report No. 11620, Haynes International, Kokomo.
4. M.F. Rothman et al., Proc. of the 9th Int. Conf. on Metallic Corrosion, Toronto, Canada, 1984
5. Haynes International, Unpublished Research.
6. H. J. Grabke, R. Krajak, E. M. Muller-Lorenz and S. Strauss, “Metal Dusting of Nickel-Base Alloys”, Materials and Corrosion, 47, (1996), p495.
7. D. L. Klarstrom, H. J. Grabke and L. D. Paul, “The Metal dusting Behavior of Several High Temperature Nickel Based Alloy,” Paper No. 01379, NACE Corrosion 2001, NACE International, Houston, TX.
8. H. J. Grabke, E. M. Muller-Lorenz, J. Klower and D. C. Agarwal, “Metal Dusting of Nickel-Based Alloys,” Materials Performance, 38, (1998), p 58.
9. B. A. Baker, G. D. Smith, V. W. Hartmann, L. E. Shoemaker and S. A. McCoy, “Nickel-Base Material Solutions to Metal Dusting Problems,” Paper No. 02394, Corrosion 2002, NACE International, Houston, TX.

10. N. Birks and G.H. Meier, Introduction to High Temperature Oxidation of Metals, Pg. 10-30, Edwin Arnold, London, 1983.
11. P. Kofstad, High Temperature Corrosion, Pp. 428-464, Elsevier Applied Science, NewYork, 1988.
12. T.P. Levi, J.F. Norton and W.T. Bakker, Materials and Corrosion, 50, 405-416 (1999).
13. S. K. Srivastava and J.E. Barnes, Sulfidation Data for Various High Temperature Alloys (Report 1), Technical File # 14675, Haynes International, 2003.
14. P. Elliot, A.A. Ansari and R. Nabovi in “High Temperature Corrosion in Energy Systems”, Ed. By M.F. Rothman, P. 437, TMS 1985
15. M.J. McNallan, et al., Paper No. 11, Corrosion 85, NACE, Houston
16. S Thongtem et al., Paper No. 372, Corrosion 86. NACE, Houston
17. P. Elliot et al., Paper No. 13, Corrosion 85, NACE, Houston
18. C. Schwalm and M. Schutze, Materials and Corrosion 51, 34-49 (2000), Ibid. Pp. 73-79, Ibid. Pp. 161-172.
19. J.J. Barnes, Paper No. 446, Corrosion 96, NACE, Houston
20. G.Y. Lai, M.F. Rothman and D.E. Fluck, CORROSION 85, Paper No. 14, NACE, Houston.
21. J.W. Slusser, J.B. Titcomb, M.T. Heffelfinger and B.R. Dunbobbin, Journal of Metals, July 1985, pp. 24 – 27

Table 1: Nominal compositions of alloys resistant to high temperature corrosion

FAMILY	ALLOY	UNS NO.	COMPOSITION, wt.% (values denoted with * are maxima, and ** are minima)											
			Ni	Co	Mo	Cr	Fe	W	Mn	Si	C	Al	Ti	OTHER
Ni-Cr	600	N06600	76	-	-	15.5	8	-	0.5	0.2	0.08	-	-	Cu 0.2
	602CA	N06025	BAL.	-	-	25	9.5	-	0.1*	0.5*	0.2	2.1	0.15	Cu 0.1* Y 0.09 Zr 0.06
	625	N06625	61	-	9	21.5	2.5	-	0.2	0.2	0.05	0.2	0.2	Nb + Ta 3.6
	671	-	BAL.	-	-	48	-	-	-	-	0.05	-	0.35	-
	690	N06690	58**	-	-	29	9	-	0.5*	0.5*	0.05*	-	-	Cu 0.5*
	693	N06693	BAL.	-	-	29	4.25	-	-	0.5*	0.15*	3.25	-	Nb 1.5
	214	N07214	75	2*	0.5*	16	3	0.5*	-	0.2*	0.04	4.5	-	Y 0.01
Ni-Cr-Mo	S	N06635	67	2*	15	16	3*	1*	0.5	0.4	0.02*	0.25	-	Cu 0.35* La 0.02 B 0.015*
Ni-Cr-W	230	N06230	57	5*	2	22	3*	14	0.5	0.4	0.1	0.3	-	La 0.02
Ni-Co-Cr	HR-160	N12160	37	29	1*	28	2*	1*	0.5	2.75	0.05	0.4*	0.5	-
	263	N07263	52	20	6	20	0.7*	-	0.4	0.2	0.06	0.6*	2.4*	Cu 0.2*
	617	N06617	52	12.5	9	22	1	-	-	0.5	0.07	1.2	0.3	-
Ni-Cr-Fe	X	N06002	47	1.5	9	22	18	0.6	-	1*	0.1	0.5*	-	-
	45-TM	N06045	45**	-	-	27.5	23	-	1*	2.75	0.09	0.2*	-	Cu 0.3* Rare Earths 0.1
	601	N06601	60.5	-	-	23	15	-	-	0.5*	0.1*	1.4	-	-
Ni-Fe-Cr	HR-120	N08120	37	3*	1*	25	33	-	-	0.6	0.05	0.5*	-	Nb 0.7 N 0.2
	800H	N08800	32.5	-	-	21	39.5**	-	1.5*	1*	0.1*	0.4	0.4	Cu 0.75*

Table 2. Oxidation in flowing air for 1008 hours, cycled to room temperature every 168 Hours

Alloy	Average Metal Affected, µm			
	980°C	1095°C	1150°C	1205°C
214	5	3	8	18
230	18	33	86	201
600	23	41	74	213
617	33	46	86	318
601	33	66	135	191
X	23	69	147	>899

Table 3. Effect of cycle time on oxidation in flowing air at 1095°C

Alloy	Average Metal affected, µm	
	168 Hr. cycle/1008 Hrs.	25 Hr. Cycle/1050 Hrs.
214	3	25
230	18	86
600	41	185
617	46	267
601	66	297

Table 4. Dynamic oxidation data with a 30 minute cycle

Alloy	Average Metal affected, µm	
	980°C/1000 Hrs.	1095°C/500 Hrs.
214	25	30
230	71	132
601	76	>610
X	142	328
617	249	>610
600	312	495

Table 5. Oxidation in flowing air for 360 days with a 30 day cycle

Alloy	Average Metal affected, µm			
	980°C	1095°C	1150°C	1205°C
214	0	0	0	36
230	64	279	874	1626
HR-120	84	589	1118	Consumed
X	71	666	1407	Consumed
HR-160	348	780	1158	1598

Table 6. Carburization Data for Nickel Alloys

Alloy	Mass Carbon Pick Up, mg/cm^2 , @ Indicated Temperature/Time		
	871°C/215 hours	927°C/215 hours	982°C/55 hours
214	0.14	0.3	0.6
263	0.1	0.4	3.8
617	0.26	2.4	5.0
625	0.31	1.1	5.3
S	0.32	1.6	2.1
600	0.40	1.3	2.8
230	0.40	2.0	2.5
X	0.45	1.8	2.5
800H	0.48	1.0	1.0
601	NA	1.8	4.8

NA = Not Available

Table 7. Carburization Data for Nickel Alloys at Low Oxygen Potential

Alloy	Mass Carbon Pick Up mg/cm^2	Avg. Int. Penetration µm	Max. Int. Penetration µm
214	0	0	0
617	2.6	383.5	419.0
HR-160	2.9	505.5	558.8
601	3.2	520.7	571.5
800H	3.6	802.6	939.8
X	5.8	525.8	558.8
230	5.8	584.2	647.7
600	7.2	1021.1	1066.8
HR-120	7.9	637.5	685.8

Table 8. Final metal wastage rates obtained for exposures In 49% CO-49% H_2-2% H_2O at 650°C

Alloy Designation	UNS No.	Total Exposure Time, Hours	Final Metal Wastage Rate, mg/cm^2h
HR-120	N08120	190	4.1×10^{-2}
800H	N08810	925	2.7×10^{-3}
214	N07214	5,707	1.0×10^{-3}
601	N06601	10,000	2.5×10^{-3}
230	N06230	10,000	3.2×10^{-4}
HR-160	N12160	10,000	0.0*

*Attack Too Small for Analysis

Table 9. Sulfidation data in a coal gasification environment at 600°C
($Ps_2 = 6.12 \times 10^{-10}$ atma, $Po_2 = 1.38 \times 10^{-25}$ atma;carbon activity = 0.18)

	2000 hr		Predicted Attack in a Year	
Alloy	Mean Metal Aff., µm	Max. Metal Aff., µm	Mean Metal Aff., µm	Max. Metal Aff., µm
HR-160	4	13	8	31
45TM	24	55	Unreliable	
MA956	9	20	19	64

Mean/Max. Metal Affected = Metal Loss + Mean/Max. Internal Attack

Table 10. Sulfidation data for nickel alloys at 760°C
($Ps_2 = 1.02 \times 10^{-07}$ atma, $Po_2 = 3.87 \times 10^{-22}$ atma; carbon activity = 0.16)

Alloy	Test Duration, hr.	Metal Loss, µm	Max. Metal Aff., µm
600	215	consumed	>551.2
601	215	consumed	>749.3
X	215	consumed	>749.3
671	215	10.2	86.4
HR-160	215	7.6	58.4

Max. Metal Affected = Metal Loss + Max. Internal Attack

Table 11. Sulfidation data for nickel alloys at 871°C
($Ps_2 = 8.11 \times 10^{-07}$ atma, $Po_2 = 1.62 \times 10^{-19}$ atma)

Alloy	Test Duration, hr.	Metal Loss, µm	Max. Metal Aff., µm
230	215	Consumed	>495.3
625	215	Consumed	>609.6
800H	215	193.0	>762.0
617	215	96.5	541.0
HR-120	215	160.0	515.6
671	215	35.6	188.0
HR-160	215	20.3	157.5
617	500	Consumed	>647.7
671	500	Consumed	>635.0
601	500	398.8	881.4
HR-120	500	452.1	1188.7
800H	500	528.3	1442.7
HR-160	500	5.1	144.8

Table 12. Sulfidation data for nickel alloys at 982°C
(Ps_2 = 4.43 x 10^{-06} atma, Po_2 = 2.24 x 10^{-17} atma)

Alloy	Test Duration, hr.	Metal Loss, µm	Max. Metal Aff., µm
230	215	83.8	>571.5
671	215	63.5	317.5
HR-160	215	63.5	210.8
800H	500	315.0	>1480.8
HR-120	500	414.0	1328.4
HR-160	500	541.0	1379.2

Table 13. Sulfidation data for nickel alloys at 1093°C
(Po_2 = 4.92 x 10^{-02} atma, Ps_2 = 3.73 x 10^{-20} atma)

Alloy	Metal Loss, µm	Max. Metal Aff., µm
230	12.7	203.2
600	12.7	127.0
X	15.2	142.2
800H	12.7	177.8
625	25.4	228.6
601	15.2	180.3
617	88.9	279.4

Table 14. Corrosion data for nickel alloys in Ar-20%O_2-0.25%Cl_2 at temperatures from 700° to 1000°C

Alloy	700°C		800°C		850°C		900°C		1000°C	
	Metal loss, µm	Total Depth, µm	Metal loss, µm	Total Depth, µm	Metal loss, µm	Total Depth, µm	Metal loss, µm	Total Depth, µm	Metal loss, µm	Total Depth, µm
214	10.2	10.2	17.8	61.0	17.8	66.0	22.9	149.9	12.7	50.8
600	-	-	20.3	86.4	38.1	132.1	127.0	251.5	330.2	386.1
601	-	-	-	-	-	-	61.0	264.2	203.2	294.6
800H	25.4	33.0	22.9	45.7	30.5	96.5	43.2	190.5	203.2	424.2
X	-	-	-	-	-	-	99.1	218.4	317.5	434.3
S	78.7	81.3	144.8	149.9	223.5	256.5	315.0	353.1	419.1	472.4
C276	33.0	45.7	66.0	71.1	162.6	175.3	299.7	345.4	419.1	449.6

Total Depth = Metal loss + Avg. Internal Attack

Table 15. Corrosion data for nickel alloys in air + 2%Cl_2

Test Temperature, °C	Alloy	Metal Loss, µm	Total Depth, µm
900°C	214	15.2	40.6
	800H	25.4	109.2
	600	50.8	127.0
	601	5.1	132.1
	625	101.6	177.8
	C-276	154.9	205.7
	230	33.0	208.3
	617	96.5	299.7
1000°C	214	25.4	50.8
	601	50.8	203.2
	800H	88.9	266.7

Table 16. Average thickness and appearance of the layers after 300 h exposure in air + 2 vol-% Cl_2

Alloy	At 300°	At 500°C	At 650°C	At 800°C
800H	1 – 2 µm pit-like, near carbides	3 – 4 µm fragile	2500 µm very buckled	75 µm buckled, fragile
45TM	1 µm pit-like, near carbides	6 µm buckled	110 µm fragile, porous, spalled in parts	110 µm little buckled, spalled in parts
690	1 – 2 µm pit-like	1 – 2 µm little porous	6 – 7 µm compact, little porous, spalled in parts	27 µm compact, little porous, spalled in parts
59	1 µm, little inward going finger like corrosion	10 µm, layer with good adherence	10 µm, continuous layer, spalled off	36 µm, porous layer, big parts had spalled off
C-2000	1 µm, no corrosion attack detectable	20 µm, layer with good adherence	105 µm, leafy layer, spalled off	590 µm, porous layer
HR-160	1 µm	1 µm, very leafy layer with cracks	20 µm, porous layer with many cracks	30 µm, porous, leafy layer
214	1 – 2 µm	7 – 8 µm, leafy layer, some internal corrosion	9 µm, slightly leafy oxide scale consisting of Cr/Fe- and Al-oxides	1 – 2 µm, leafy oxides, spallation

Table 17. Corrosion of nickel alloys in 100% HCL gas

Alloy	Test Temperature, °C	Metal Loss Rate, mm/y
Ni 201	685	4.2
600	685	7.5
HR-160	685	7.0
214	685	5.7
602CA	685	28.6
HR-160	735	45.6
Ni201	785	16.7
600	785	26.4
HR-160	785	96.0

Table 18. Field test results in NaCl-KCl-$BaCl_2$ at 840°C for 1 month

Alloy	Total Attack Depth, mm
X	0.96
S	1.02
214	1.80
600	2.44
601	>2.92

Table 19. Laboratory corrosion test results in a NaCl bath at 840°C

Alloy	Total Attack Depth, mm
601	0.066
214	0.079
X	0.097
800H	0.109
625	0.112
617	0.122
230	0.140
S	0.168
600	0.196

Table 20. Corrosion rates of nickel alloys in equimolar $NaNO_3$-KNO_3

Alloy	Corrosion Rate, mm/y	
	675°C/1920 hr	700°C/720 hr
214	0.41	0.53
600	0.25	0.99
N	0.23	1.22
601	0.48	1.25
800	1.85	6.60

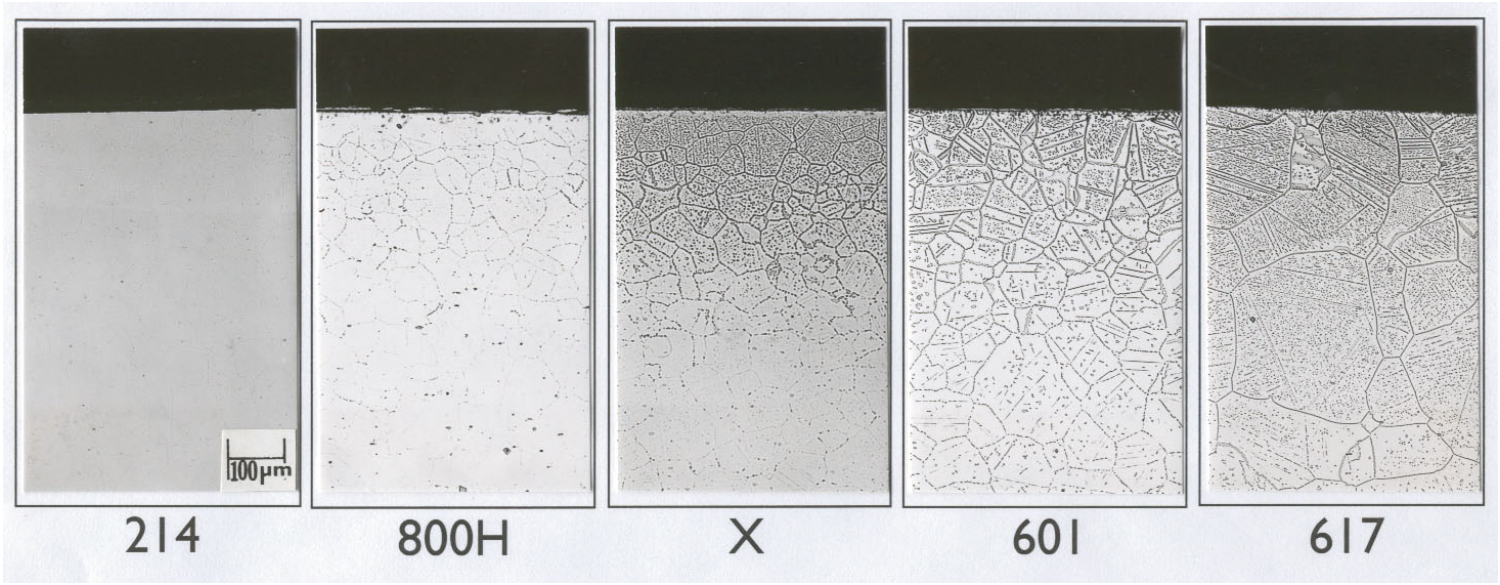

Figure 1. Carburization attack in several nickel alloys after testing at 982°C for 55 hr

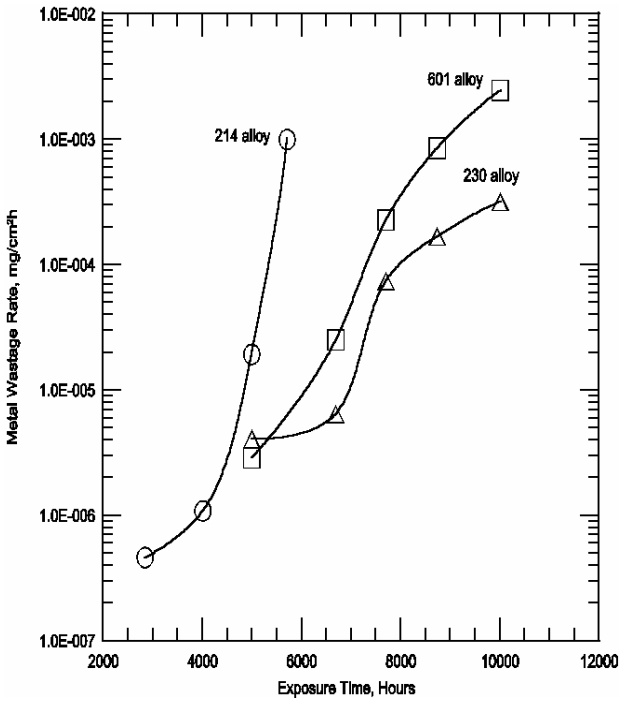

Figure 2. Metal wastage rates as a function of time In 49% CO-49%H_2-2%H_2O at 650°C.

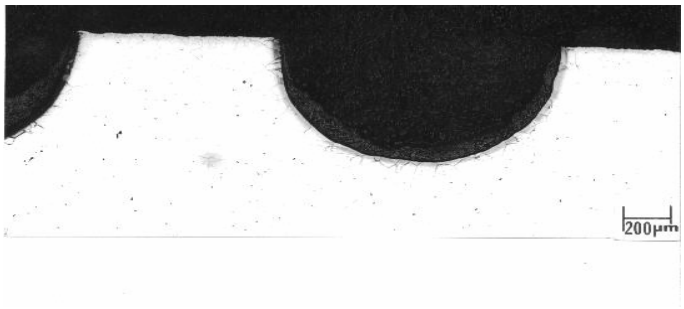

Figure 3. Metal dusting pitting attack in 601 alloy